J Comput Neurosci (2011) 30:747–758
DOI 10.1007/s10827-010-0290-z

Interplay of the magnitude and time-course of postsynaptic Ca^{2+} concentration in producing spike timing-dependent plasticity

Kristofor D. Carlson · Nicholas Giordano

Received: 29 April 2010 / Revised: 1 September 2010 / Accepted: 2 November 2010 / Published online: 1 December 2010

Abstract Synaptic strength can be modified by the relative timing of pre- and postsynaptic activity, a phenomenon termed spike timing-dependent plasticity (STDP). Studies of neurons in the hippocampus and in other regions have found that when presynaptic activity occurs within a narrow time window, typically 10 or 20 ms, before postsynaptic activity, long-term potentiation (LTP) is induced, while if presynaptic activity occurs within a similar time window after postsynaptic activity, long-term depression (LTD) results. The mechanisms underlying these modifications are not completely understood, although there is strong evidence that the postsynaptic Ca^{2+} concentration plays a central role. Some previous modeling of STDP has focused on the dynamics of the postsynaptic Ca^{2+} concentration, while other work has studied biophysical mechanisms of how a synapse can exist in, and switch between, different states corresponding to LTP and LTD. Building on previous work in these two areas we have developed the first low level STDP model of a tristable biochemical system that incorporates induction and maintenance of both LTP and LTD. Our model is able to explain the STDP observed in hippocampal neurons in response to pre- and postsynaptic pulse pairs, using only parameters derived from previous work and without the need for parameter fine-tuning. Our results also give insight into how and why the time course of the postsynaptic Ca^{2+} concentration can lead to either LTP or LTD, and suggest that voltage dependent calcium channels play a key role.

Keywords STDP · LTP · LTD · Calcium · NMDAR

Action Editor: J. Rinzel

Electronic supplementary material The online version of this article (doi:10.1007/s10827-010-0290-z) contains supplementary material, which is available to authorized users.

K. D. Carlson (✉) · N. Giordano
Department of Physics, Purdue University,
525 Northwestern Ave., West Lafayette,
IN 47907-2036, USA
e-mail: carlsokd@purdue.edu

1 Introduction

STDP is of interest for several reasons. From a general, phenomenological perspective, STDP has been used to implement efficient learning protocols in various abstract neural network models, such as those based on integrate and fire model neurons. It has been shown that an STDP learning protocol leads to several desirable properties, such as synaptic "gain control", in a natural way, and may thus be important in practical applications of neural networks (Song et al. 2000). Second, STDP is an example of Hebbian learning (Hebb 1949) which is accessible for both experiments and modeling studies (Caporale and Dan 2008). The detailed biophysical mechanism(s) elucidated through modeling of STDP may thus give deeper insight into Hebbian learning and perhaps into other learning mechanisms as well.

Many forms of LTP/LTD have been observed in the hippocampus and other brain regions which include cyclic adenosine monophosphate (cAMP)-dependent presynaptic forms of LTP (Nicoll and Malenka 1995; Linden 1997), metabotropic glutamate receptor (mGluR)-dependent LTD (Bolshakov and Siegelbaum 1994; Bender et al. 2006; Nevian and Sakmann 2006),

endocannabinoid-mediated LTD (Sjostrom et al. 2003), and N-methyl D-aspartate receptor (NMDAR) suppression induced LTD (Froemke et al. 2005). Perhaps the most studied of these forms of plasticity, however, is NMDAR-dependent LTP/LTD of excitatory synapses found in the CA1 region of the hippocampus. Our work involves the mechanisms responsible for STDP-induced early phase LTP/LTD induction and maintenance in this region. These events take place typically within the first 60 min after STDP protocols. Because late phase LTP/LTD requires protein synthesis, it occurs over a time scale of days to weeks and is outside the scope of this paper.

Experiments have led to the following general picture of NMDAR-dependent STDP-induced LTP/LTD. Channels associated with postsynaptic NMDARs open when two conditions are satisfied simultaneously: (1) when glutamate attaches to binding sites in the synaptic cleft, and (2) the postsynaptic potential is high enough to induce the removal of Mg^{2+} that blocks the associated channels in the resting state. Glutamate is released into the cleft when an action potential reaches the presynaptic side, while the elevated postsynaptic potential is usually presumed to be caused by a back-propagating action potential (BPAP) although an elevated postsynaptic potential may be producd in other ways (Lisman and Spruston 2005). Hence, the two requirements for the opening of NMDARs involve both pre- and postsynaptic events.

The opening of NMDARs produces an influx of Ca^{2+}, and it is believed that the elevated postsynaptic calcium concentration causes a switching between synaptic states. Experiments show that either LTP or LTD can result, depending on the relative timing of the pre- and postsynaptic pulses. Experiments have also revealed that voltage-dependent calcium channels (VDCCs) play an important role, and that the inhibition of VDCC activity tends to suppress LTD (Bi and Poo 1998).

Although there are different forms of LTP and LTD expression, much work has been done to show an important mechanism for changing synaptic efficacy in early LTP/LTD is an increase or decrease in the number of α-amino-3-hydroxy-5-methyl-4-isoxazolepropionic acid receptors (AMPARs) in the synaptic membrane via activity dependent changes in AMPAR trafficking (Bredt and Nicoll 2003; Malenka and Nicoll 1999; Malinow and Malenka 2002; Lee et al. 2002; Lin et al. 2000; Luthi et al. 1999; Man et al. 2000). Other mechanisms responsible for changing synaptic efficacy in early LTP/LTD have been observed and play a role in LTP/LTD expression such as the modulation of AMPAR function via a phospho/dephosphorylation cycle at sites S831 and S845 on the GluR1 subunit of the AMPARs (Castellani et al. 2001, 2005, 2009). Although it is beyond the scope of our model, it is worth noting that late phase LTP has different maintenance mechanisms than that of early phase LTP such as the splitting of the spine into two distinct synapses and new spine growth (Abraham and Williams 2003; Yuste and Bonhoeffer 2001). Although both late phase LTP and LTD require protein synthesis (Pittenger and Kandel 2003; Sajikumar and Frey 2003), much less is known about late phase LTD. In our work we will assume that changes in synaptic efficacy occur via changes in AMPAR trafficking although this is not an essential part of our model.

Modeling of STDP has been carried out by several groups at varying levels of detail. “High level” modeling of STDP includes phenomenological approaches where explicit modeling of BPAPs, neuronal potentials, ion channels, chemical networks and other low level biophysical phenomena are replaced by modeling more general variables that represent the net effects of these underlying mechanisms or by applications of a “learing rule” that changes synaptic strength by a simple factor that is a function of the time delay between pre- and postsynaptic spikes (Gerstner et al. 1996; Van Rossum et al. 2000; Pfister and Gerstner 2006). Intermediate level modeling of STDP often includes a detailed description of the neuron, including its internal voltage, ion channels, BPAPs, and internal Ca^{2+} dynamics, with the descriptions of synaptic plasticity due to mechanisms such as AMPAR trafficking or AMPAR phosphorylation left as higher level abstract equations (Karmarkar and Buounomano 2002; Abarbanel et al. 2003; Rubin et al. 2005; Shouval et al. 2002; Hartely et al. 2006). Finally, “low level” models of STDP explicitly include descriptions of neuronal parameters and plasticity mechanisms (Graupner and Brunel 2007; Urakubo et al. 2008). Our work is aimed at constructing such a low level model of STDP that identifies specific synaptic changes that can lead to LTP and LTD, and shows how these changes are produced by the interplay of pre- and postsynaptic activity.

Our model of STDP explicitly includes neuronal parameters and plasticity mechanisms. Our work is similar in spirit to that by Graupner and Brunel (2007) who provided a detailed model that showed how STDP protocols can be combined with bistable chemical switches to reproduce STDP experimental data. There is experimental evidence showing that depotentiation is fundamentally different from LTD (Zhuo et al. 1999). A tristable switch may be required to appropriately describe LTP and LTD (Pi and Lisman 2008). We combine compartmental modeling of the postsynaptic

neuron (Shouval et al. 2002) and the calcium dynamics created from STDP protocols with a tristable kinase/phosphatase network (Pi and Lisman 2008). Our model reproduces experimental data from Bi and Poo (1998) showing good qualitative agreement for both pulse pair protocols and the blockade of L-type VDCCs protocol. To our knowledge, our model is the only one that pairs both STDP-induced postsynaptic calcium dynamics with a tristable biochemical switch and is able to yield an LTP state, an LTD state, and a basal synaptic state. Our model is also unique in being an STDP model that accounts for both early LTP/LTD induction and maintenance phases (Pi and Lisman 2008).

2 Materials and methods

2.1 Overview of the Model

A biophysical model of STDP must contain at least two primary ingredients. The first is a mechanism through which the synaptic strength can exist in at least three different states, corresponding to the basal state, the LTP state, and the LTD state. An appealing model of a multistate synapse involves biochemical switches, as developed in several systems and described by Bhalla and coworkers (Bhalla and Iyengar 1999). For our work, we adopt the tristable biochemical network described by Pi and Lisman (2008), which involves CaMKII and PP2A on the postsynaptic side of the synapse. Lisman and coworkers have shown how this system can have three stable states: a basal state with low concentrations of both phosphorylated CaMKII (henceforth denoted pK) and dephosphorylated PP2A (denoted P), an LTP state with high pK and low P, and an LTD state with low pK and high P. Switching between these states is controlled by the calcium concentration (denoted by Ca). These states are self-sustaining; once the system moves into one of these states, it remains there when Ca returns to basal levels. While possessing interesting biophysical properties, some important aspects of the Lisman model that are relevant for STDP have not yet been explored. In particular, the behavior of the model when subjected to relatively short bursts of calcium, as occurs in STDP, has not been studied previously. Such studies will be described below.

The second key part of a model of STDP is a description of the Ca dynamics. Switching between synaptic states is triggered by the postsynaptic Ca^{2+} concentration, so a model of Ca^{2+} dynamics is required to obtain a complete description of STDP. The generally accepted picture of this process is that calcium enters the postsynaptic region mainly through NMDARs and VDCCs. This picture has been developed and studied by Shouval et al. (2002) and by Rubin et al. (2005), and our treatment of the Ca^{2+} current largely follows those studies.

In this paper, we show that a combination of the Lisman model of synaptic switching and the NMDAR/VDCC picture of calcium dynamics does, in fact, give a good description of the observed STDP in response to pairs of pre- and postsynaptic pulses. We show how the concentration and time course of Ca together determine the switching behavior of the Lisman model. Specifically, we find that the increase in the Ca^{2+} concentration is temporally longer when the BPAP arrives before glutamate binding, and that this makes conditions favorable for LTD. We also show that the temporal scales associated with the CaMKII/PP2A network and in the Ca^{2+} dynamics combine to give a time window for STDP that agrees well with experimental studies of STDP, and that the presence of VDCCs is crucial for LTD. The insights gained from our studies of the STDP induced by pulse pairs will be important for understanding and modeling STDP for more complicated pulse protocols (triplets, spike bursts, etc.), a problem that remains to be fully understood.

2.2 Calcium dynamics

The postsynaptic side of the synapse is modeled as a single equipotential compartment with both NMDARs and VDCCs present as sources of Ca^{2+} influx, and a decay term that drives the Ca^{2+} concentration toward basal levels to account for buffering. The calcium current due to NMDARs is given by (Shouval et al. 2002)

$$I_{NMDA}(V,t) = P_0 \cdot G_{NMDA} \cdot \theta_1(t) \cdot [I^f_{\text{glut}} e^{(t_{\text{glut}}-t)/\tau^f_{\text{glut}}} + I^s_{\text{glut}} e^{(t_{\text{glut}}-t)/\tau^s_{\text{glut}}}] \cdot H(V) \quad (1)$$

where V is the postsynaptic potential and glutamate is released at a time $t = t_{\text{glut}}$. Here $P_0 = 0.5$ is the fraction of NMDARs that change to the open state after glutamate binding and $G_{NMDA} = 1.75$ mS/cm^2 is the conductance of the open NMDARs from Ca^{2+} ions. These values were determined using data from Sabatini et al. (2002) for increases in the postsynaptic Ca^{2+} concentration due to NMDAR currents, along with single channel conductance measurements for NMDARs and NMDAR densities reported by Wolf et al. (2005) and Dalby and Mody (2003). The values of other parameters in Eq. (1) were taken from Shouval

et al. (2002) and are given in the supplementary materials at http://www.springer.com/biomed/neuroscience/journal/10827.

The exponential factors in Eq. (1) describe the time course of glutamate unbinding. This binding is taken to be instantaneous and is accounted for in Eq. (1) by the step function $\theta_1(t)$ where

$$\theta_1(t) = \begin{cases} 0, & t < t_{\text{glut}} \\ 1, & t > t_{\text{glut}} \end{cases} \tag{2}$$

Glutamate unbinding is characterized by two decay constants, $\tau^f_{\text{glut}} = 50$ ms and $\tau^s_{\text{glut}} = 200$ ms (Shouval et al. 2002; Carmignoto and Vicini 1992), and the exponential factors in Eq. (1) give a decrease in the Ca^{2+} current as time passes and glutamate unbinds. The fast and slow unbinding components I^f_{glut} and I^s_{glut} both have values of 0.5.

The term $H(V)$ describes Mg^{2+} unblock due to changes in the postsynaptic potential. Following Jahr and Stevens (1990) we take

$$H(V) = (V_{\text{Ca}} - V)/(1 + ([Mg^{2+}]/3.57)e^{-62 \cdot V}) \tag{3}$$

Where $V_{\text{Ca}} = 130$ mV is the reversal potential of calcium (Shouval et al. 2002), $[Mg^{2+}] = 1.5$ mM is the external magnesium ion concentration, and V in Eq. (3) is in mV.

We use a simple implementation of the VDCC current with

$$I_{VDCC}(V,t) = G_{VDCC} \cdot \theta_2(V,t) \cdot (V_{VDCC} - V) \tag{4}$$

with

$$\theta_2(V,t) = \begin{cases} 1, & V > -30 \text{ mV and } t_{\text{bpap}} + 2\text{ms} > t > t_{\text{bpap}} \\ 0, & \text{otherwise} \end{cases} \tag{5}$$

where the BPAP begins at $t = t_{\text{bpap}}$. The maximal VDCC conductance is $G_{VDCC} = 0.80$ mS/cm^2 and the Ca^{2+} reversal potential $V_{VDCC} = 130$ mV is the same as that used in Eq. (3). This value of G_{VDCC} was chosen so that opening of the VDCCs gives an increase in the postsynaptic Ca^{2+} concentration equal to that reported in experiments by Sabatini et al. (2002). The time course of a BPAP is determined by the function $\theta_2(V,t)$ which effectively opens the VDCC for an interval of 2 ms beginning at t_{bpap}, which is the time when the BPAP is initiated. In principle, the time course of a BPAP could have been calculated using a biophysical dendritic model with Na^+ and K^+ currents, a realistic model for the dendritic geometry, etc. However, we suggest that STDP should be robust in the sense that the precise details of how V varies during the BPAP should not be a crucial factor, and hence that the very simple description of the VDCC current in Eqs. (4) and (5) should be adequate when BPAPs are well separated in time, as they are in our studies of the behavior with pre- and postsynaptic pulse pairs.

While the precise time dependence of a BPAP is not crucial for determining I_{VDCC}, it is needed for modeling the Mg^{2+} unblock through the function $H(V)$. We follow the work of Shouval et al. (2002) and take the BPAP voltage to have the form

$$V_{\text{bpap}}(t) = V_{\max}\left[\left(I^f_{\text{bpap}} e^{-(t-t_{\text{bpap}})/\tau^f_{\text{bpap}}}\right) + \left(I^s_{\text{bpap}} e^{-(t-t_{\text{bpap}})/\tau^s_{\text{bpap}}}\right)\right], \tag{6}$$

with parameter values taken again from Shouval et al. The fast and slow components have amplitudes of $I^f_{\text{bpap}} = 0.75$ and $I^s_{\text{bpap}} = 0.25$ with time constants $\tau^f_{\text{bpap}} = 3$ ms and $\tau^s_{\text{bpap}} = 25$ ms, and the maximum amplitude is $V_{\max} = 100$ mV.

The NMDA and VDCC currents (Eqs. (1) and (4)) describe the flow of Ca^{2+} into the postsynaptic side. This removal is modeled with a simple exponential decay so the total rate of change of Ca is

$$\frac{dCa}{dt} = I_{NMDA} + I_{VDCC} - \frac{Ca - Ca_{\text{basal}}}{\tau_{\text{decay}}}. \tag{7}$$

The basal concentration of Ca^{2+} is taken to be $Ca_{\text{basal}} = 0.1$ μM (Shouval et al. 2002) while the decay constant is $\tau_{\text{decay}} = 12$ ms (Sabatini et al. 2002) (although we note that values of τ_{decay} as high as 80 ms have been reported; Markram et al. 1995).

2.3 Lisman model of the CaMKII/PP2A network

Our modeling of the CaMKII/PP2A reaction network exactly follows the work of Pi and Lisman (2008). The postsynaptic Ca^{2+} concentration affects the rates of autocatalytic reactions that convert CaMKII and PP2A from their nonphosphorylated to phosphorylated forms. For CaMKII the concentration of the phosphorylated form, which is the active form, is denoted by pK, while for PP2A the nonphosphorylated form is active, and its concentration is denoted by P. All equations describing the evolution of pK and P were taken directly from Pi and Lisman (see the supplementary material for details). According to the Lisman model, the values of pK and P govern AMPA receptor trafficking which determines the number of receptors inserted in the postsynaptic membrane and hence the synaptic efficacy. Pi and Lisman also describe a model of how the concentration of AMPARs depends on pK and P. The model is capable of only three

AMPAR levels, so their model yields only full LTP and full LTD. No graded response is possible with this model and the same is true of the modeling results we describe in this paper. The synaptic strength can have only three possible values: basal, LTP, and LTD.

2.4 Implementation

Our calculations were implemented in C, with the differential equations expressed as difference equations and solved using the Euler method (Giordano and Nakanishi 2005). Two stimuli act as triggers for flow of Ca^{2+}: a presynaptic action potential which releases glutamate into the synaptic cleft and a BPAP that increases the postsynaptic potential. Given a specified time interval between glutamate release and the BPAP, the variation of the postsynaptic Ca^{2+} concentration, and the values of pK and P were calculated as functions of time.

3 Overview of the model: assumptions and goals

Our model has many ingredients and makes many assumptions, and it is useful to be clear on the limitations that these imply. It is also important to be clear on what we hope to learn from the study of this model. In short, the questions we wish to answer include: (1) If we combine the established picture of the Ca^{2+} current associated with NMDARs (Eq. (1)) and a simple model of the Ca^{2+} current associated VDCCs (Eq. (4)), with the tristable biochemical switch contained in the Lisman model of CaMKII/PP2A, can we explain both the LTP and LTD found in STDP? (2) The NMDARs provide one "coincidence" detector that effectively senses the relative timing of pre- and postsynaptic activity. Can this one coincidence detector control both LTP and LTD, or do we need a second coincidence detector, as suggested by Karmarkar and Buonomano (2002) (3) Some modeling work relies on just the postsynaptic Ca^{2+} concentration (Shouval et al. 2002), and such a description generally assumes that small levels of Ca^{2+} will lead to LTD. This picture seems to then lead automatically to LTD when the presynaptic pulse occurs long before the postsynaptic pulse, but this does not appear to be found in many experiments. Can our model explain why LTD is not found in this case? (4) Experiments show that the inhibition of VDCCs suppresses LTD; why is this the case? We will see that our model can explain all of these observations and answer all of these questions.

Since our model involves many parameters and equations, we have tried to keep the model as simple as possible and avoid the tuning of parameters. For example, we have adopted the entire model of the CaMKII/PP2A network discussed by Pi and Lisman (2008), using all of the parameters they have found in their studies. Likewise, we have adopted the mathematical descriptions of NMDARs and VDCCs given by previous workers. We have used a very simple description of VDCCs and BPAPs, which should capture their essential time dependences. We could, of course, give more Hodgkin-Huxley-like treatments of both of these parts of the model, but that would not change the basic time dependence of the VDCC current or the BPAP, so we have chosen to employ the simpler descriptions (Eqs. (4) and (7)) used here. In addition, a better description of synaptic strength, including AMPA trafficking, etc., could be given, but is not required to address the basic questions listed in the previous paragraph. Our model can be improved in various ways, but such improvements are not needed to tackle these basic questions.

Finally, we note that other models of STDP have explored or suggested essential roles for effects not included in our model, such as allosteric kinetics of NMDA receptors (Urakubo et al. 2008), more realistically generated BPAPs (Graupner and Brunel 2007; Urakubo et al. 2008), nano-domain Ca^{2+} interactions with CaMKII activation near NMDAR and VDCC channels (Lee et al. 2009), and AMPAR modulation via phosphorylation (Castellani et al. 2009). Some or all of these may well be important in STDP, but they are not part of the central question addressed in our work: can a simple description of NMDARs and VDCCs together with the Lisman model of CaMKII/PP2A account for the essential properties STDP?

4 Results

4.1 Synaptic switching of the CaMKII/PP2A network

Switching between the basal, LTP, and LTD synaptic states occurs when the postsynaptic compartment is exposed to an elevated calcium concentration. In STDP, this calcium influx has a complicated time course described by Eq. (1) (the NMDAR current), 4 (the VDCC current), and 7 (calcium update). To better understand the resulting synaptic switching, it is useful to consider how the CaMKII/PP2A network responds in simpler situations. To this end, we have studied the behavior of the Lisman CaMKII/PP2A network in response to a simple calcium "pulse" with an amplitude of A_{Ca} and a duration T_{Ca}. In these calculations, the system began in the basal state at $t = 0$. The calcium pulse was then

applied for a period T_{Ca}, and the state of the system was determined at times long after the pulse ended. The final state of the CaMKII/PP2A system was then found to be stable in either the LTP state, LTD state, or basal state. Figure 1 shows results for two different values of T_{Ca}. The results for $T_{Ca} = 500$ ms (Fig. 1(a) and (b)) are consistent with those reported by Pi and Lisman (2008). For the relatively small calcium amplitude ($A_{Ca} = 2.2$ μM; Fig. 1(b)) the system switched into the LTD state. This is indicated by the large value of P (the dephosphorylated PP2A concentration) and the low value of pK (the phosphorylated CaMKII concentration) when the calcium concentration returned to basal levels. The large value of P is maintained indefinitely (calculations not shown here) by the autocatalytic nature of the CaMKII/PP2A network. For the larger calcium amplitude ($A_{Ca} = 4.0$ μM; Fig. 1(a)) the system switched into the LTP state, indicated by the large value of pK and the small value of P at long times. This large value of pK was stable; i.e., was maintained indefinitely, even after Ca returned to its basal level.

It should be noted that experiments indicate that elevations in active forms of CaMKII and PP2A eventually return to basal levels within an hour after the STDP protocols (Barria et al. 1997; Thiels et al. 1998). New research has shown, however, that CaMKII activation may be elevated for only a few minutes (Lee et al. 2009) after some STDP protocols. This may still be enough time for AMPAR trafficking to take place due to rapid delivery of AMPARs to silent synapses previously lacking AMPARs during LTP expression (Malinow and Malenka 2002). For this to occur there must be a pool of readily available non-synaptic AMPARs near the synapse, which has been observed experimentally (Shi et al. 1999). During the time window for LTP/LTD expression via AMPAR trafficking to occur, the active forms CaMKII/PP2A remain activated for long past our simulation duration of 20 s.

Figure 1(c) and (d) show corresponding results for a much shorter application of calcium, $T_{Ca} = 30$ ms. This shorter application of calcium is most relevant for STDP, since the values of most of the time constants in Eq. (1) (the NMDAR current) and Eq. (4) (the VDCC current) are less than 100 ms. In this case we find that a large amplitude Ca pulse again results in LTP (Fig. 1(c)), but that a small amplitude pulse results in the basal state, and not LTD, as found for a longer pulse with the same value of Ca.

The results in Fig. 1 show that the behavior of the CaMKII/PP2A network depends on both the amplitude and the duration of the applied calcium. To investigate this behavior in more detail, we have studied a wide range of values of A_{Ca} and T_{Ca}. The results are

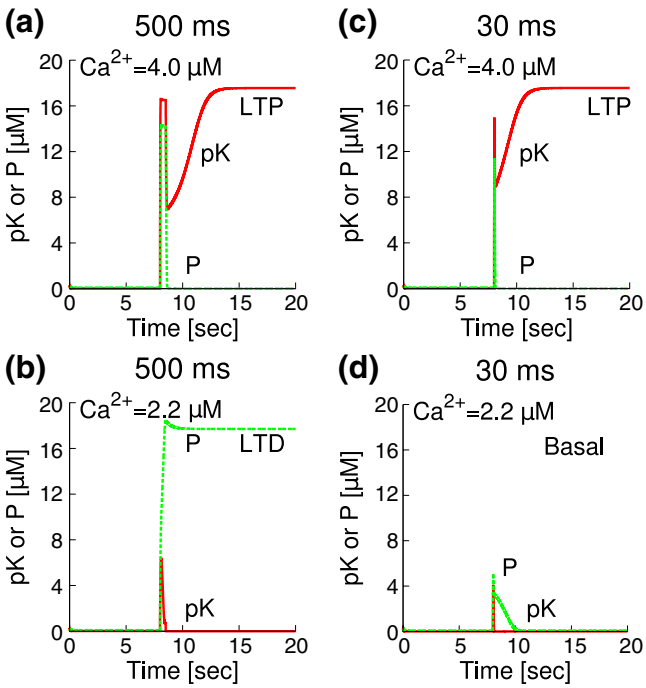

Fig. 1 Pi and Lisman (2008) showed how the tristable CaMKII/PP2A chemical network can attain stable states when Ca^{2+} is applied for 2 s. Here we consider shorter timescales. (**a**) and (**b**), show simulation results, for 500 ms applications of 4.0 μM and 2.2 μM of calcium, respectively. Tristability is achieved, similar to that found by Pi and Lisman. The results in (**c**) and (**d**) show that tristability cannot be attained with only a 30 ms application of Ca^{2+} (Note that (**c**) demonstrates LTP while (**d**) shows that LTD does not occur)

shown in the form of a "final state diagram" in Fig. 2, with the final states being the basal, LTP, and LTD states.

Figure 2(a) shows the behavior for relatively long T_{Ca}. In broad terms, LTD is found for calcium pulses with an amplitude below about 3 μM, LTP is found for pulses with amplitudes between about 3 μM and 5.5 μM, and the basal final state is found for larger calcium concentrations. A more complex picture is found when the behavior is examined for T_{Ca} below 100 ms, in Fig. 2(b). Here we see that LTD is only found when the duration T_{Ca} is longer than about 45 ms, while LTP can occur when the duration is greater than about 10 ms.

The results in Fig. 2 show how the final state of the CaMKII/PP2A network depends on both the magnitude and the duration of the calcium pulse. This point has been made in previous modeling work (Pi and Lisman 2008; Rubin et al. 2005), but the results presented here are more detailed than previous reports. Our results show that LTP is favored at moderate to high calcium levels, while LTD is favored at low calcium levels. Just as important, LTD requires

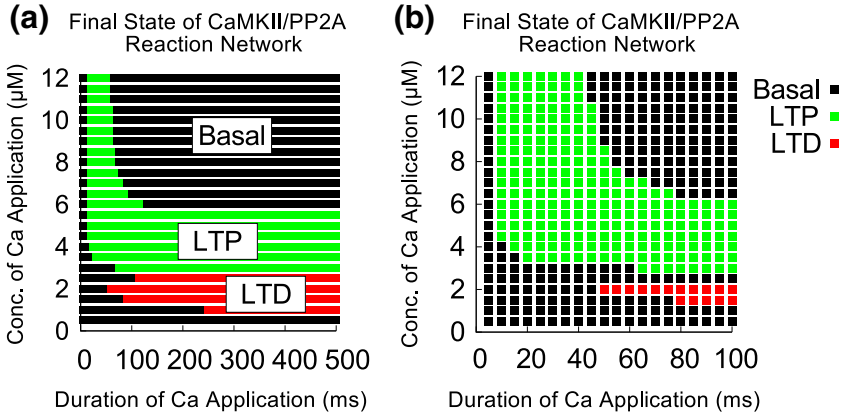

Fig. 2 (**a**) Final state of the CaMKII/PP2A reaction network as a function of the amplitude A_{Ca} (*vertical axis*) and duration T_{Ca} (*horizontal axis*) of an applied calcium pulse. These states are stable indefinitely, even after the calcium concentration returns to its basal level. The different regions appear "jagged" because the calculations were performed on a finite grid of values for both the duration and calcium amplitude. (**b**) Final state diagram showing the behavior for the short duration times most relevant for STDP

significantly longer applications of calcium than LTP. These results will be very helpful in understanding several aspects of STDP, including the role of VDCCs.

4.2 Qualitative picture of the induction of LTP and LTD

We next consider synaptic switching in response to postsynaptic calcium levels produced by NMDARs (Eq. (1)), VDCCs (Eq. (4)), and reuptake (Eq. (7)), which are triggered by pre- and postsynaptic activity. The time course of the postsynaptic calcium concentration produced by these three mechanisms is more complex than the simple pulses considered in Figs. 1 and 2, but we will see that the general conclusions drawn from Fig. 2 will still apply.

The overall picture is as follows. LTP induction begins with a presynaptic release of glutamate that subsequently binds to postsynaptic NMDARs. At some time Δt later, a postsynaptic BPAP causes an increase in the postsynaptic voltage, relieving the Mg^{2+} block of the NMDARs at the opening of these channels, producing an influx of calcium according to Eq. (1). The BPAP also causes the opening of VDCCs (Eq. (4)) giving an additional, but somewhat smaller calcium influx. The net result is a large increase in the postsynaptic calcium concentration, which activates the CaMKII switch leading to a large value of pK. This large value of pK inhibits the PP2A switch from activating PP2A further, and the system enters into the LTP state. Finally, the increased pK concentration causes an increased number of AMPARs in the postsynaptic membrane giving an increase in synaptic conductance resulting in LTP. Since this chain of events is triggered when presynaptic activity occurs before postsynaptic activity, we refer to this case as "pre-before-post".

The induction of LTD begins with a BPAP. This BPAP causes VDCCs to open and a moderate increase in calcium in the postsynaptic compartment. NMDARs remain closed because they require both glutamate binding and postsynaptic depolarization, but glutamate is not yet present in the cleft. Some time Δt later, presynaptic activation occurs, releasing glutamate which binds to the NMDARs. If the postsynaptic side is still sufficiently depolarized from the tail of the BPAP, the NMDARs will open, causing additional calcium influx. The net calcium influx in this case is moderate and persists for a longer period as compared to that found in the pre-before-post case. This moderate increase in calcium activates the PP2A switch, resulting in an increase in P, which then inhibits the CaMKII switch and drives the system to the LTD state. This increases the rate of AMPAR removal from the postsynaptic membrane, causing a decrease in synaptic conductance resulting in LTD. Since this chain of events is triggered when presynaptic activity occurs after postsynaptic activity, we refer to this case as "pre-after-post".

4.3 Time dependence of Ca, pK, and P during LTP and LTD

We next consider the time course of postsynaptic calcium produced by NMDARs and VDCCs as a result of pre- and postsynaptic activity. We define the time delay between presynaptic activation and postsynaptic activation as

$$\Delta t = t_{\text{post}} - t_{\text{pre}} = t_{\text{bpap}} - t_{\text{glut}} \,, \tag{8}$$

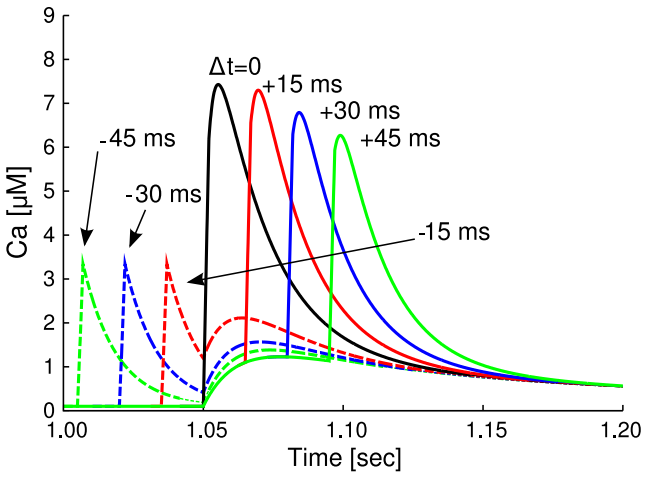

Fig. 3 The pre-before-post case ($\Delta t > 0$) produces a relatively narrow increase in *Ca* concentration, while the pre-after-post case ($\Delta t < 0$) produces a smaller elevation in *Ca* concentration. A large rise in *Ca* tends to activate the CaMKII pathway, while a prolonged, modest *Ca* increase is more likely to activate the PP2A pathway. At long times, *Ca* returns to its basal level

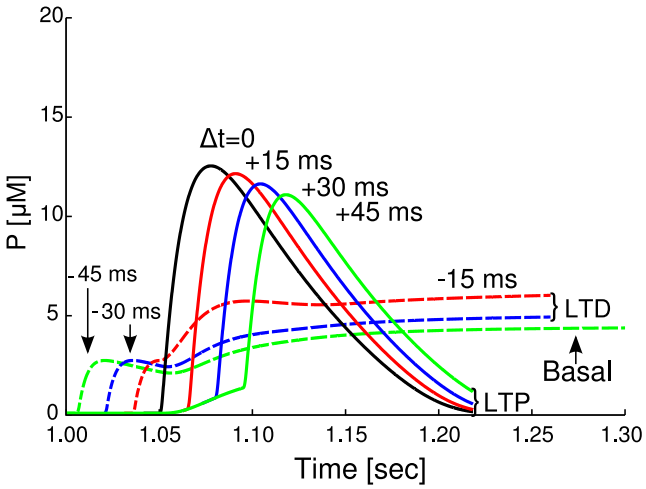

Fig. 5 The pre-after-post ($\Delta t < 0$) case keeps *P* concentrations elevated even after the *Ca* concentration returns to basal levels, leading to LTD. The pre-before-post ($\Delta t > 0$) case fails to keep *P* concentrations elevated and thus does not lead to LTD expression. Note that when $\Delta t < -45$ ms, the system eventually returns to basal levels at very long times (not shown here). Neither LTP or LTD is found in this case

Δt is thus positive when the presynaptic side is activated first (pre-before-post), and negative when the presynaptic side is activated after the postsynaptic side (pre-after-post). The behavior of *Ca* for various values of Δt are shown in Fig. 3, while Figs. 4 and 5 show the corresonding results for pK and *P*, all as functions of time.

We first consider the LTP regime ($\Delta t \geq 0$). In this regime there is a large peak in the calcium concentration (Fig. 3), as both the NMDARs and the VDCCs open. As Δt increases, the peak amplitude of *Ca* decreases. This peak in *Ca* produces a corresponding peak in pK (Fig. 4), and for the cases with $\Delta t \geq 0$ shown here, the value of pK remains high after the NMDARs and VDCCs have closed and *Ca* has returned to its basal level. In this regime *P* exhibits a peak when *Ca* is high (Fig. 5), but *P* returns to a low level when the calcium concentration returns to its basal level. The system has thus switched to the LTP state.

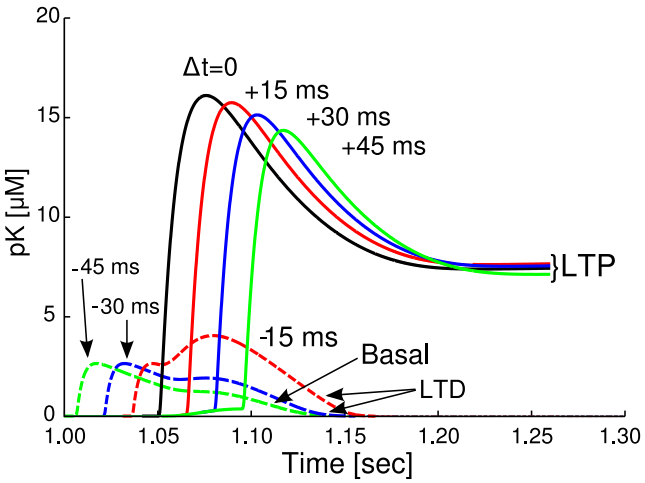

Fig. 4 The pre-before-post ($\Delta t > 0$) case keeps pK concentrations elevated even after the *Ca* concentration returns to basal levels, leading to LTP. The pre-after-post ($\Delta t < 0$) cases fail to keep pK concentrations elevated and thus do not lead to LTP expression

We next consider the LTD regime ($\Delta t < 0$), the results for which are shown as dashed curves in Figs. 3–5. In this regime *Ca* exhibits two peaks, with the first peak produced by the opening of VDCCs when the BPAP arrives, and the second peak occuring when NMDARs open. When $|\Delta t|$ is not too large, these two peaks overlap and give a general *Ca* increase that persists longer and has a smaller amplitude than in the LTP regime. This is just what is needed to activate the PP2A switch (Fig. 2). The behavior of *P* in Fig. 5 shows that this does indeed occur; the value of *P* remains large and well above the basal value long after the calcium influx ends, and while pK drops to its basal level when *Ca* falls back to basal levels. The system has thus switched into the LTD state. When the BPAP occurs well before the presynaptic activity, that is, when Δt is large and negative, the calcium influx from the VDCCs and the NMDARs are well separated in time (see the curve in Fig. 3 for $\Delta t = -45$ ms) and the increase in the calcium concentration is not sufficiently large or long to induce LTD. This is understandable in terms of the dynamic response of the CaMKII/PP2A switch in Fig. 2.

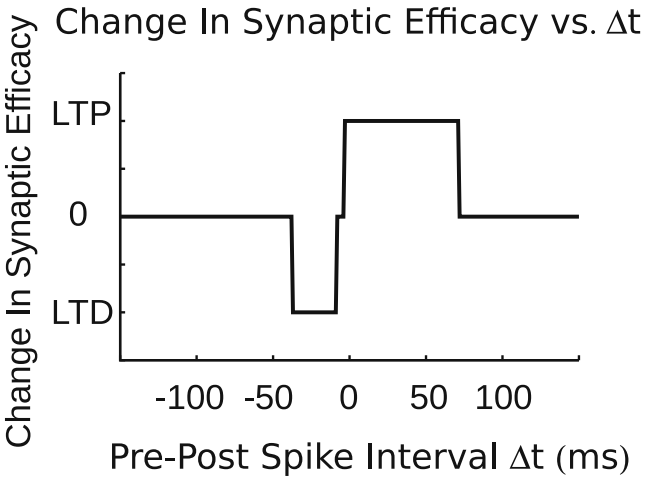

Fig. 6 Change in synaptic efficacy as a function of Δt for the full model. Δt is positive when the presynaptic activity occurs before the postsynaptic activity. These changes in efficacy are stable indefinitely. A value of zero on the vertical scale represents the basal state; i.e., no change in synaptic strength

The behavior for different values of Δt are collected in Fig. 6, where we show the final state of the CaMKII/PP2A network as a function of Δt. The vertical axis gives the change in synaptic strength; a positive change corresponds to LTP, a negative change to LTD, and a change of zero corresponds to the basal state.

Figure 6 shows that LTP occurs for positive values of Δt up to about $\Delta t \approx 75$ ms, while LTD is found for negative values of Δt to a limit of about $\Delta t \approx -30$ ms. There is also a very small region near $\Delta t \approx 0$ where the basal state is found. Outside the range -30 ms $\leq \Delta t \leq 75$ ms the system remains in the basal state. These results for the limits at which LTD occurs agree well with the experiments Bi and Poo (1998). This range for which LTP is found appears to be a bit larger than found in experiments (Bi and Poo 1998; Markram et al. 1997). Possible reasons for this discrepancy will be discussed below. We also note that, in agreement with the experiments of Bi and Poo, our model does not exhibit LTD at large positive values of Δt. This is a regime in which the amplitude of the Ca^{2+} peak is moderate, and hence from Fig. 1 one might have expected to observe LTD. The model of Shouval et al. (2002), which treats only the Ca^{2+} dynamics and not the complex interplay of CaMKII and PP2A, does, in fact, predict such behavior. The reason why our model does not predict LTD in this regime can be traced to the relatively narrow *Ca* peak in this case. The Ca^{2+} concentration is not elevated long enough to cause the CaMKII/PP2A network to switch to the LTD state, in analogy with the results in Fig. 2.

Our computational model has STDP induction behavior different from experimental observations. Experimental results show that successful LTP/LTD induction requires many pulses (60) at a frequency of 1 Hz (Bi and Poo 1998; Wang et al. 2005) yet our model shows successful LTP/LTD induction with only one spike pairing. The purpose of our model is to explain the general behavior of STDP induced LTP/LTD using the most basic assumptions and biophysical mechanisms possible. Although it may be possible to replicate this observation by parameter tuning such as modifying CaMKII/PP2A sensitivity to Ca^{2+} or ion channel conductance, such calculations are left for later models as it is not the scope of this paper.

4.4 Role of VDCCs

Experimental results from Bi and Poo (1998) show that blocking VDCCs abolishes LTD and reduces the magnitude of LTP. We therefore also studied the behavior of our model with the calcium current from VDCCs omitted; the results are shown in Fig. 7, where we show the change in synaptic strength as a function of Δt.

We now find that switching to the LTP state only occurs for $0 \leq \Delta t \leq 25$ ms, suggesting that while LTP does still occur, it is less robust than when the VDCCs are present. When Δt was negative (pre-after-post), the system switches into the LTD state only over the narrow range -15 ms $\leq \Delta t \leq -4$ ms. The LTD regime

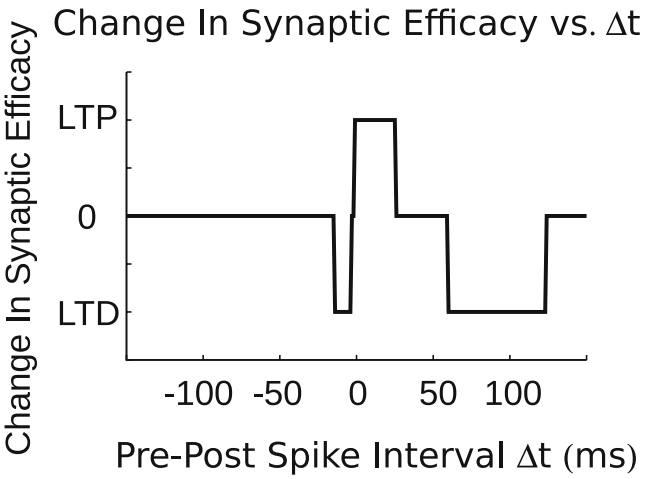

Fig. 7 Change in synaptic efficacy as a function of Δt, with the VDCCs inhibited. Δt is positive when the presynaptic activity occurs after the postsynaptic activity. These changes are stable indefinitely. A value of zero on the vertical scale represents the basal state; i.e., no change in synaptic strength. Note that LTD is now found for large positive values of Δt, unlike the behavior when the VDCCs are not inhibited

is thus also significantly smaller than when the VDCCs are not inhibited. Both of these results are in accord with the experiments of Bi and Poo (1998). We also find that pre-before-post time intervals in the range 50 ms $\leq \Delta t \leq 120$, result in LTD. This behavior (the possibility of which has been noted and discussed previously by Shouval et al. 2002) can be understood by considering the phase diagram in Fig. 2(b). For these values of $\Delta t > 0$ the calcium influx from both NMDARs and VDCCs (assuming they are not blocked) has an amplitude and duration that tends to switch the system into the LTP regime. When the VDCCs are blocked the calcium influx is smaller, and we have already seen from the phase diagram in Fig. 2 that this can cause the system to switch instead into the LTD state. This is indeed found in Fig. 7 when 50 ms $< \Delta t <$ 120 ms. For larger values of Δt the calcium concentration is not large enough to switch out of the basal state, while for smaller values of Δt the calcium duration is large enough and long enough to result in LTP. We do not know of any experimental evidence for LTD in this regime when VDCCs are blocked; it will be interesting if future experiments can explore this range in more detail.

5 Discussion

Any successful model of STDP must contain several basic features. The first is a tristable system in which the synaptic efficacy can assume one of three possible states: basal, LTP, and LTD. (Here we leave aside the question of a graded synaptic synaptic response, which, as noted above, cannot be described by the model of AMPAR trafficking used in our work.) The model we have studied contains the chemical network studied by Pi and Lisman (2008), which exhibits three stable fixed points when the Ca^{2+} concentration is at its basal level, corresponding to the basal, LTP, and LTD synaptic states.

Second, a model of STDP must contain some way of detecting the relative timing of pre- and postsynaptic activity, and responding accordingly. Our model accomplishes this coincidence detection using a combination of mechanisms. One is based on NMDARs, which open only when both glutamate binding is triggered by presynaptic activity, and Mg^{2+} block is simultaneously removed by postsynaptic activity. The other mechanism relies on the dynamics of the CaMKII/PP2A reaction network and its response to changes in the Ca^{2+} concentration. Our simulations show that this coincidence detector can respond appropriately to pre-before-post and pre-after-post intervals in the range of tens of milliseconds, as observed in studies of STDP. This coincidence detector is sensitive to the time order of pre- and postsynaptic activity, so there is no need to posit separate coincidence detectors for the pre-before-post and pre-after-post cases, as some other modeling work has suggested (Karmarkar and Buonomano 2002; Urakubo et al. 2008). We also find that inhibiting VDCCs reduces the time ranges over which LTP and LTD occur, again in good agreement with experimental studies. This is an important result from our model.

Quantitatively, our model gives a fairly good account of the major aspects of STDP, although the ranges of Δt that result in LTP and LTD are somewhat wider than found experimentally. We believe that this level of agreement of the model with experiments on STDP is quite satisfactory, since the results presented in this paper have been obtained using only parameters which have been suggested by previous modeling work, or that have been inferred directly from experimental studies. No parameter values have been "tuned" to improve agreement with studies of STDP. It will be interesting to study how these ranges depend on the parameters that control the time scales and amplitudes of the calcium currents resulting from NMDARs and VDCCs.

Examination of the dynamics of Ca^{2+} influx gives important insights into the mechanism of STDP in our model. In the regime of LTP, the Ca^{2+} influxes from NMDARs and VDCCs are coincident, giving a relatively large but short increase in the postsynaptic Ca^{2+} concentration. This causes the CaMKII/PP2A network to switch to the LTP state, in which the phosphorylated CaMKII concentration is high. In the regime of LTD, the NMDARs and VDCCs open at different times giving a smaller but longer increase in the postsynaptic Ca^{2+} concentration. This causes a switch to the LTD state, in which the dephosphorylated PP2A concentration is high. The response of the CaMKII/PP2A network to both the amplitude and the duration of the Ca^{2+} influx demonstrates how a single coincidence detector can respond in two different ways, leading to either LTP or LTD. It also explains why a long pre-before-post interval does not cause a switch to the LTD state, which was a difficulty found in some models as discussed by Shouval et al. (2002).

While our model successfully accounts for STDP in situations involving a single presynaptic spike paired with a single postsynaptic spike, there are many other spike protocols that remain to be explored with the model, including triplets/quadruplets (Wang et al. 2005) and presynaptic bursts paired with voltage-clamped postsynaptic neurons (Kelso et al. 1986; Malinow and Miller 1986). As mentioned earlier,

changes in the Lisman CaMKII/PP2A biochemical network such as changing sensitivity of CaMKII/PP2A to Ca^{2+} may reproduce experimental evidence showing that many spike pairings are required for LTP/LTD induction (Bi and Poo 1998; Wang et al. 2005) instead of the single spike pair induced LTP/LTD we observed in our model. The CaMKII/PP2A biochemical network may also need to be modified to reproduce experimental data showing that CaMKII and PP2A do not remain in their active forms indefinitely (Barria et al. 1997; Thiels et al. 1998; Lee et al. 2009). Finally, computational models that allow for a graded synaptic response, AMPAR modulation via phosphorylation of AMPAR subunits, and a more realistic treatment of BPAPs by more accurately modeling the ion channels involved in generating action potentials deserve further study.

References

Abarbanel, H. D. I., Gibb, L., Huerta, R., & Rabinovich, M. I. (2003). Biophysical model of synaptic plasticity dynamics. *Biological Cybernetics, 89*, 214–226.

Abraham, W. C., & Williams, J. M. (2003). Properties and mechanisms of LTP maintenance. *Neuroscientist, 9*, 463–474.

Barria, A., Muller, D., Derkach, V., Griffith, L. C., & Soderling, T. R. (1997). Regulatory phosphorylation of AMPA-type glutamate receptors by CaMKII during long-term potentiation. *Science, 276*, 2042–2045.

Bender, V. A., Bender, K. J., Brasier, D. J., & Feldman, D. E. (2006). Two coincidence detectors for spike timing-dependent plasticity in somatosensory cortex. *Journal of Neuroscience, 26*, 4166–4177.

Bhalla, U. S., & Iyengar, R. (1999). Emergent properties of networks of biological signaling pathways. *Science, 283*, 381–387.

Bi, G. Q., & Poo, G. (1998). Synaptic modifications in cultured hippocampal neurons: Dependence on spike timing, synaptic strength, and postsynaptic cell type. *Journal of Neuroscience, 18*, 10464–10472.

Bolshakov, V. Y., & Siegelbaum, S. A. (1994). Postsynaptic induction and presynaptic expression of hippocampal long-term depression. *Science, 264*, 1148–1152.

Bredt, D. S., & Nicoll, R. A. (2003). AMPA receptor trafficking at excitatory synapses. *Neuron, 40*, 361–379.

Carmignoto, G., & Vicini, S. (1992). Activity-dependent decrease in NMDA receptor responses during development of the visual cortex. *Science, 258*, 1007–1011.

Caporale, N., & Dan, Y. (2008). Spike timing-dependent plasticity: A hebbian learning rule. *Annual Review of Neuroscience, 31*, 25–46.

Castellani, G. C., Bazzani, A., & Cooper, L. N. (2009). Toward a microscopic model of bidirectional synaptic plasticity. *Proceedings of the National Academy of Science of the United States of America, 106*, 14091–14095.

Castellani, G. C., Quinlan, E. M., Bersani, F., Cooper, L. N., & Shouval, H. Z. (2005). A model of bidirectional synaptic plasticity: From signaling network to channel conductance. *Learning and Memory, 12*, 423–432.

Castellani, G. C., Quinlan, E. M., Cooper, L. N., & Shouval, H. Z. (2001). A biophysical model of bidirectional synaptic plasticity: Dependence on AMPA and NMDA receptors. *Proceedings of the National Academy of Science of the United States of America, 98*, 12772–12777.

Dalby, N. O., & Mody, I. (2003). Activation of NMDA receptors in rat dentate gyrus granule cells by spontaneous and evoked transmitter release. *Journal of Neurophysiology, 90*, 786–797.

Froemke, R. C., Poo, M. M., Dan, Y. (2005). Spike-timing-dependent synaptic plasticity depends on dendritic location. *Nature, 434*, 221–225.

Gerstner, W., Kempter, R., Van Hemmen, J. L., & Wagner, H. (1996). A neuronal learning rule for sub-millisecond temporal coding. *Nature, 383*, 76–78.

Giordano, N. J., & Nakanishi, H. (2005). *Computational physics* (2nd Ed.). Saddle River: Prentice-Hall.

Graupner, M., & Brunel, N. (2007). STDP in bistable synapse model based on CaMKII and associated signaling pathways. *PloS Computational Biology, 3*, 2299–2323.

Hartley, M., Taylor, N., & Taylor, J. (2006). Understanding spike-time-dependent plasticity: A biologically motivated computational model. *Neurocomputing, 69*, 2005–2016.

Hebb, D. O. (1949). *The organization of behavior*. New York: Wiley.

Jahr, C. E., & Stevens, C. F. (1990). Voltage dependence of NMDA-activated macroscopic conductances predicted by single-channel kinetics. *Journal of Neuroscience, 10*(9), 3178–3182.

Karmarkar, U. R., & Buonomano, D. V. (2002). A model of spike-timing dependent plasticity: One or two coincidence detectors? *Journal of Neurophysiology, 88*, 507–513.

Kelso, S. R., Ganong, A. H., & Brown, T. H. (1986). Hebbian synapses in hippocampus. *Proceedings of the National Academy of Science of the United States of America, 83*, 5326–5330.

Lee, S. H., Liu, L., Wang, Y. T., & Sheng, M. (2002). Clathrin adaptor AP2 and NSF interact with overlapping sites of GluR2 and play distinct roles in AMPA receptor trafficking and hippocampal LTD. *Neuron, 36*, 661–674.

Lee, S. R., Escobedo-Lozoya, Y., Szatmari, E. M., & Yasuda, R. (2009). Activation of CaMKII in single dendritic spines during long-term potentiation. *Nature, 458*, 299–306.

Lin, J. W., Ju, W., Foster, K., Lee, S. H., Ahmadian, G., Wyszynski, M., et al. (2000). Distinct molecular mechanisms and divergent endocytotic pathways of AMPA receptor internalization. *Nature Neuroscience, 3*, 1282–1290.

Linden, D.J. (1997). Long-term potentiation of glial synaptic currents in cerebellar culture. *Neuron, 18*, 983–994.

Lisman, J., & Spruston, N. (2005). Postsynaptic depolarization requirements for LTP and LTD: A critique of spike timing-dependent plasticity. *Nature Neuroscience, 8*, 839–841.

Luthi, A., Chittajallu, R., Duprat, F., Palmer, M. J., Benke, T. A., Kidd, F. L., et al. (1999). Hippocampal LTD expression involves a pool of AMPARs regulated by the NSF-GluR2 interaction. *Neuron, 24*, 389–399.

Malenka, R. C., & Nicoll, R. A. (1999). Long-term potentiationa decade of progress? *Science, 285*, 1870–1874.

Malinow, R., & Malenka, R. C. (2002). AMPA receptor trafficking and synaptic plasticity. *Annual Review of Neuroscience, 25*, 103–126.

Malinow, R., & Miller, J. P. (1986). Postsynaptic hyperpolarization reversibly blocks induction of long-term potentiation. *Nature, 320*, 529–530.

Man, H. Y., Lin, J. W., Ju, W. H., Ahmadian, G., Liu, L., Becker, L. E., et al. (2000). Regulation of AMPA receptor-mediated synaptic transmission by clathrin-dependent receptor internalization. *Neuron, 25*, 649–662.

Markram, H., Helm, P. J., & Sakmann, B. (1995). Dendritic calcium transients evoked by single back-propagating action potentials in rat neocortical pyramidal neurons. *Journal of Physiology, 485*, 1–20.

Markram, H., Lubke, J., Frotscher, M., & Sakmann, B. (1997). Regulation of synaptic efficacy by coincidence of postsynaptic APs and EPSPs. *Science, 275*, 213–215.

Nevian, T., & Sakmann, B. (2006). Spine Ca2+ signaling in spike-timing-dependent plasticity. *Journal of Neuroscience, 26*, 11001–11013.

Nicoll and Malenka(1995). Contrasting properties of two forms of long-term potentiation in the hippocampus. *Nature, 377*, 115–118.

Pfister, J. P., & Gerstner, W. (2006). Triplets of spikes in a model of spike timing-dependent plasticity. *Journal of Neuroscience, 26*, 9673–9682.

Pi, H. J., & Lisman, J. E. (2008) Coupled phosphatase and kinase switches produced the tristability required for long-term potentiation and long-term depression. *Journal of Neuroscience, 28*, 13132–13138.

Pittenger, C., & Kandel, E. R. (2003). In search of general mechanisms for long-lasting plasticity: Aplysia and the hippocampus. *Philosophical Transactions of the Royal Society of London B Biological Sciences, 358*, 757–763.

Rubin, J. E., Gerkin, R. C., Bi, G. Q., & Chow, C. C. (2005). Calcium time course as a signal for spike timing-dependent plasticity. *Journal of Neurophysiology, 93*, 2600–2613.

Sabatini, B. L., Oertner, T. G., & Svoboda, K. (2002). The life cycle of Ca^{2+} ions in dendritic spines. *Neuron, 33*, 439–452.

Sajikumar, S., & Frey, J. U. (2003). Anisomycin inhibits the late maintenance of long-term depression in rat hippocampal slices *in vitro*. *Neuroscience Letters, 338*, 147–150.

Shi, S. H., Hayashi, Y., Petralia, R. S., Zaman, S. H., Wenthold, R. J., Svoboda, K., et al.(1999). Rapid spine delivery and redistribution of AMPA receptors after synaptic NMDA receptor activation. *Science, 284*, 1811–1816.

Shouval, H. Z., Bear, M. F., & Cooper, L. N. (2002). A unified model of NMDA receptor-dependent bidirectional synaptic plasticity. *Proceedings of the National Academy of Science of the United States of America, 99*, 10831–10836.

Sjostrom, P. J., Turrigiano, G. G., & Nelson, S. B. (2003). Neocortical LTD via coincident activation of presynaptic NMDA and cannabinoid receptors. *Neuron, 39*, 641–654.

Song, S., Miller, K. D., & Abbott, L. F. (2000). Competitive hebbian learning through spike-timing dependent synaptic plasticity. *Nature Neuroscience, 3*, 919–926.

Thiels, E., Norman, E. D., Barrionuevo, G., & Klann, E. (1998). Transient and persistent increases in protein phosphatase activity during long-term depression in the adult hippocampus *in vivo*. *Neuroscience, 86*, 1023–1029.

Urakubo, H., Honda, M., Froemke, R. C., & Kuroda, S. (2008). Requirement of an allosteric kinetics of NMDA receptors for spike timing-dependent plasticity. *Journal of Neuroscience, 28*, 3310–3323.

Van Rossum, M. C. W., Bi, G. Q., & Turrigiano, G. G. (2000). Stable hebbian learning from spike timing dependent plasticity. *Journal of Neuroscience, 20*, 8812–8821.

Wang, H. X., Gerkin, R. C., Nauen, D. W., & Bi, G. Q. (2005). Coactivation and timing-dependent integration of synaptic potentiation and depression. *Nature Neuroscience, 8*, 187–194.

Wolf, J. A., Moyer, J. T., & Finkel, L. H. (2005). The role of NMDA currents in state transitions of the nucleus accumbens medium spiny neuron. *Neurocomputing, 65–66*, 565–570.

Yuste, R., & Bonhoeffer, T. (2001). Morphological changes in dendritic spines associated with long-term synaptic plasticity. *Annual Review of Neuroscience, 24*, 1071–1089.

Zhuo, M., Zhang, W., Son, H., Mansuy, I., Sobel, R. A., Seidman, J., et al. (1999). A selective role of calcineurin aalpha in synaptic depotentiation in hippocampus. *Proceedings of the National Academy of Science of the United States of America, 96*, 4650–4655.